

Numerical Analysis and Design of Wing-Body Configuration Based on Busemann Biplane

*D. Maruyama**, *M. Yonezawa***, *K. Kusunose****, *K. Matsushima***** and *K. Nakahashi**

**Tohoku University, Department of Aerospace Engineering*

Aoba-ku, Aramaki-Aza-Aoba 6-6-01, Sendai, Japan

***Tohoku University, Institute of Fluid Science*

Aoba-ku, Katahira 2-1-1, Sendai, Japan

****Formerly, Tohoku University, Institute of Fluid Science*

Aoba-ku, Katahira 2-1-1, Sendai, Japan

Currently, Ministry of Defense, Technical Research and Development Institute

Sakae-cho, 1-2-10, Tachikawa, Japan

*****University of Toyama, Department of Mechanical Engineering*

3190 Gofuku, Toyama, Japan

Abstract

Busemann biplane is known as the representative of an airfoil configuration that has possibility of reducing wave drag and sonic boom. This abstract should indicate aerodynamic performance of supersonic biplane wings that are attached to a body. In this paper, analyses of supersonic biplanes and wing-body configurations are discussed based on Computational Fluid Dynamics (CFD). We investigated aerodynamic performance of the wings in Euler simulations with changes of the positions where the wings are attached to the body. When supersonic biplane wings are affected by the expansion waves generated from the body, aerodynamic performance of the wings is improved at the cruise condition. Furthermore, the unstating Mach number, which is the Mach number at which flow choking occurs when a biplane wing decelerates from its design Mach number, is reduced from 1.63 to 1.60.

1. Introduction

For practical design of a wing-body configuration based on the concept of Busemann biplane in the future, some fundamental studies on interference effects of bodies with supersonic biplane wings are necessary. Kusunose and Odaka proposed a wing-body configuration that generates strong shock waves and expansion waves to assume the condition that supersonic biplane wings are strongly affected by those waves [1-3]. They confirmed that a supersonic biplane wing without winglet has possibility of realizing better aerodynamic performance when it is affected by expansion waves from the body.

In this paper, we investigate aerodynamic performance of biplane wings when they are affected by a body. Therefore, only the aerodynamic performance of supersonic biplane wings is discussed. The cruise Mach number is 1.7. Two types of supersonic biplane wings are applied to the body proposed by Kusunose and Odaka. The sectional configurations and planforms of these two wings are identical. The difference is only whether a winglet is on the wingtip. The sectional configuration is a Busemann biplane, whose total thickness-chord ratio is 0.10. The planform parameters of these wings are as follows: the taper ratio is 0.25, the reference area is 1, the aspect ratio is 5.12 and the mid-chord line is normal to the free-stream direction. These are fixed in this paper.

As a first step of investigation of the interference effects, some wing-body configurations are analyzed with changes of the positions where the wings are attached to the body. These are simulated at the cruise conditions, and also at off-design conditions to investigate unstating problems on deceleration stages because the unstating problems are important for the stability around the cruise condition.

2. Aerodynamic characteristics of isolated wings

First of all, we discuss isolated supersonic biplane wings. In this paper, the flow solver named TAS code [4-7] was used for flow analyses. In this paper, all analyses were simulated using the Euler equations and conducted using a three-dimensional unstructured mesh. Figure 1 shows orthographic drawing, mesh and C_p visualizations of a tapered Busemann biplane wing. The sectional configuration of the wing is a Busemann biplane. The thickness-chord ratio (t/c) of each element of the configuration is 0.05, therefore, 0.10 in total. The gap between its two elements (h/c) is 0.505. These are identical at all span stations. The mid-chord line of the wing is normal to the free-stream direction. Table 1 shows planform parameters of the tapered biplane wing. This tapered wing has better aerodynamic performance area than the two-dimensional airfoil that has the same configuration as the sectional one of the tapered biplane wing (this can be confirmed in Fig. 3).

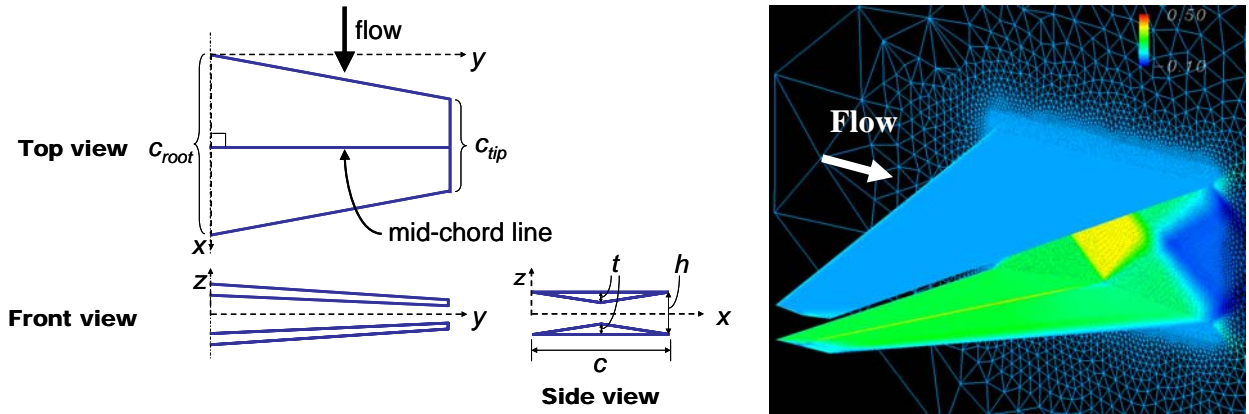


Figure 1: Orthographic drawing, mesh and C_p visualizations of a Busemann biplane wing with taper planform

Table 1 : Planform parameters of a Busemann biplane wing as a baseline model

parameter	value
taper ratio	0.25
aspect ratio	5.12
semi-span length	1.6
reference area	1

As can be observed in Fig. 1, there exist an inappropriate area of interaction of shock waves and expansion waves around the wingtip. This is due to wingtip effects and it produces increase of C_D . A winglet was introduced to the biplane wing in order to reduce C_D due to the wingtip effects. Figure 2 shows C_p and mesh visualizations of a Busemann biplane wing without a winglet and the one with a winglet. The former is the identical wing with that shown in Fig. 1. Table 2 shows drag coefficients of these biplane wings. The winglet can reduce C_D , eliminating the wingtip effects. Figure 3 shows spanwise C_d distributions of these two wings. We discuss these characteristics by dividing the spanwise area into three domains as shown in Fig. 3. Domain1 is a high drag domain. The high drag is caused by Mach cones from the wing root. Domain2 is a low drag domain. The C_D s at this domain are lower than that of the two-dimensional airfoil. This is the unique characteristics on tapered biplane wings. At Domain3 the two biplane wings are quite different in aerodynamic characteristics. The drag increase due to the Mach cones from the wingtip is observed on the biplane without winglet. The opposite characteristics to that at Domain1 are observed on the biplane with winglet. Both the drag increase at Domain1 and the decrease at Domain3 are due to mirror effects. That is why the drags of the biplane wing with winglet at Domain3 are quite low. Although there is an anxiety of increase of skin friction due to increase of the area, the winglet is effective for supersonic biplanes by above-mentioned advantages. In the following chapters, these two biplane wings (Busemann biplane without winglet and Busemann biplane with winglet) are used as wings of wing-body configurations treated later.

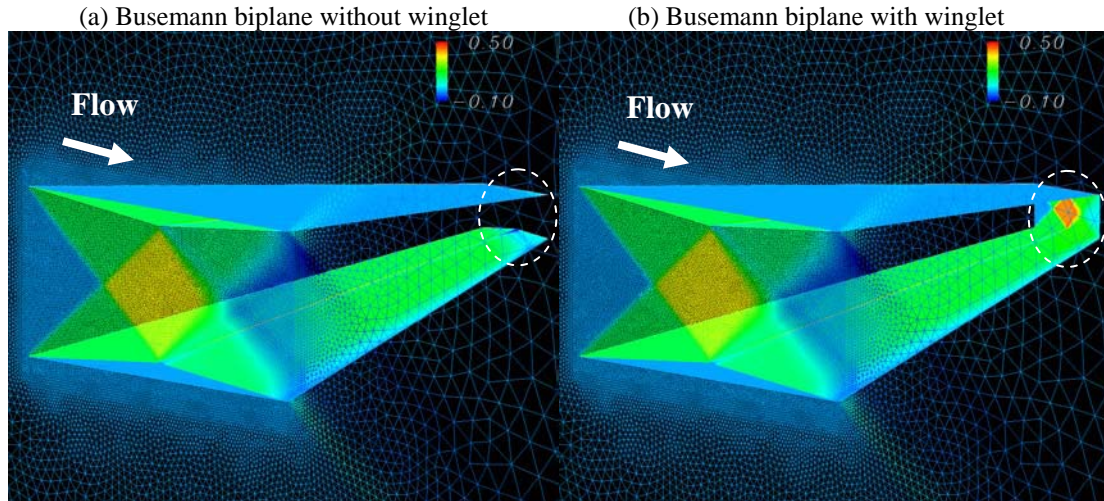


Figure 2: C_p and mesh visualizations of tapered Busemann biplane wings

Table 2 : Drag coefficients of Busemann biplane wings without winglet and with winglet at zero-lift conditions

	C_D
without winglet	0.00326
with winglet	0.00283

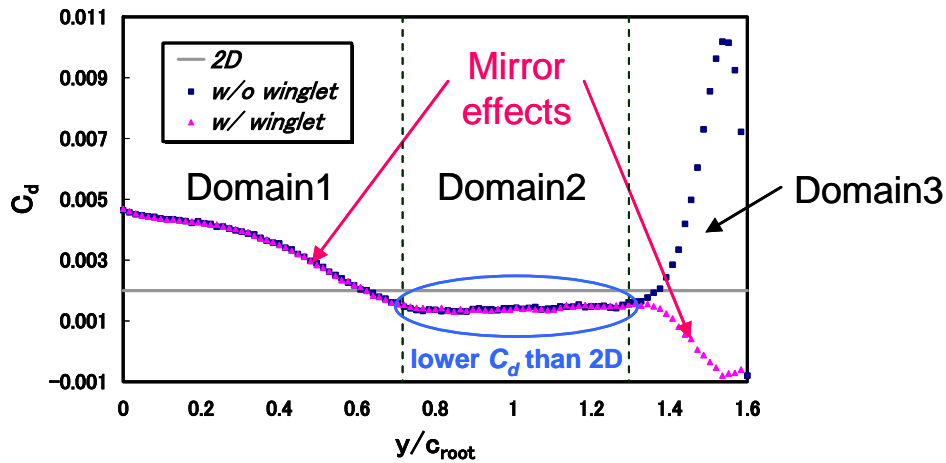


Figure 3: Spanwise C_d distributions of a tapered Busemann biplane wing without a winglet and the one with a winglet

3. Analysis of wing-body configurations using Busemann biplane

The goal of our study is to propose a practical supersonic transport using the biplane concept. As a first step of this study, interference effects between a supersonic biplane wing and a body (fuselage) was investigated. In this chapter, wing-body configurations are simulated aerodynamically and aerodynamic performance of wings of the wing-body configurations is analyzed and discussed at their design (cruise) conditions.

3.1 Wing-body configurations

A wing-body configuration proposed by Odaka and Kusunose [1-3] was adopted to investigate wave interference effects. Figure 4 shows the wing-body configuration proposed by them. The body has a conical configuration at the nose and a rectangular parallelepiped at the back. It generates strong shock waves from its nose and also generates expansion waves. The wing of the wing-body configuration is attached to the body so that Mach cones generated by

the nose of the body can influence the whole area of the wing. Here, the wing configuration of the wing-body configuration is the Busemann biplane wing without winglet shown in the previous chapter (see Fig. 1 and Table 1). Figure 5 shows C_p visualization of the wing-body configuration at $z=0$ simulated by Odaka and Kusunose. It has been already shown by Odaka and Kusunose that aerodynamic performance of the biplane wing of the wing-body configuration is higher than that of the isolated wing at the cruise condition.

In this study, two types of supersonic biplane wings discussed in the previous chapter are applied for the wing-body configuration. One is the Busemann biplane without winglet (see Fig. 2(a)). The other is the Busemann biplane with winglet (see Fig. 2(b)). These are termed ‘isolated w/o wlt’ and ‘isolated w/ wlt’, respectively. Under these conditions, four cases of positions where the wings are attached to the body are investigated. Therefore, there are eight types of wing-body configurations in total. An overview of positions where the wings are attached to the body are shown in Fig. 6. Here, x_w means the distance in x -wise from the nose to the mid-chord line of a wing. These wing-body configurations are discussed compared with the above-mentioned isolated wings.

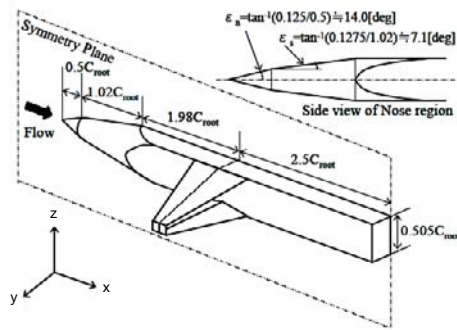


Figure 4: Simple diagram of a wing-body configuration proposed by Odaka and Kusunose [Refs. 1-3]

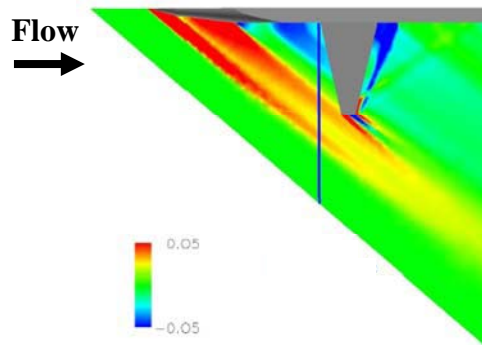


Figure 5: C_p visualization at $z=0$ of the wing-body configuration simulated by Odaka and Kusunose [Refs. 1-3]

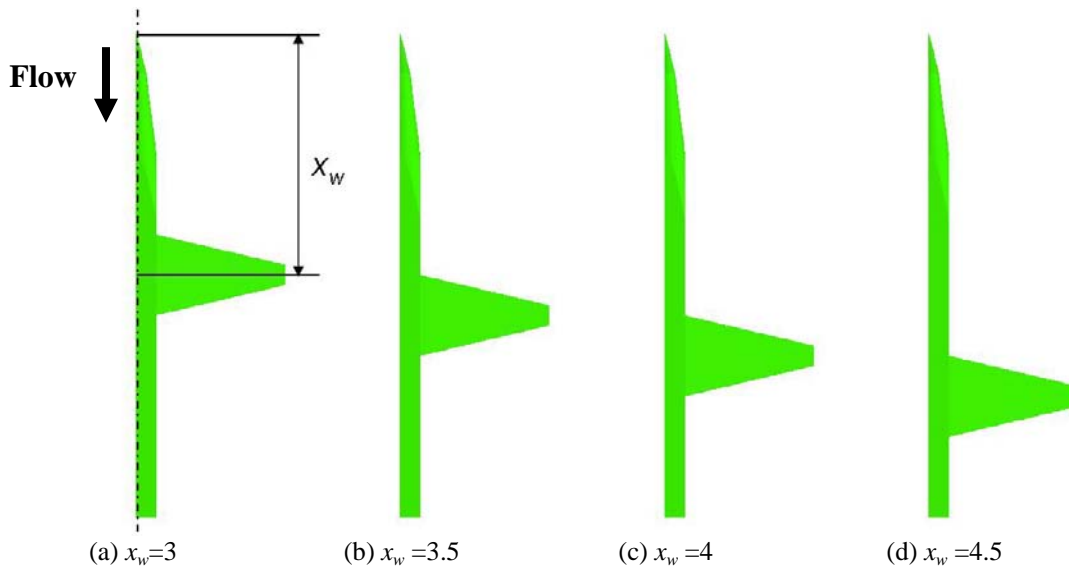


Figure 6: An overview of positions where a wing is attached to a body

3.2 Aerodynamic performance at cruise condition

We discuss aerodynamic performance of the wings of the wing-body configurations at their design conditions. Figure 7 shows a mesh visualization used for analysis at the cruise condition. The number of nodes of each wing-body configuration is about 2.0 million. Figure 8 shows C_p visualization at $z=0$ of each wing-body configuration. Only cases of “w/ wlt (with winglet)” are described here to show flow fields with shock waves and expansion waves generated from each body. When $x_w=3$ and 3.5, the wings are affected strongly by compression waves generated from the nose of the body and also affected by expansion waves from the body. On the other hand, when $x_w=4$ and 4.5, they are exposed by only the expansion waves. The wings of the wing-body configurations w/o wlt are affected by the waves from the body as well. Figure 9 shows drag polar curves of the wings of the wing-body configurations w/o wlt and w/ wlt compared to the isolated wings. On both w/o wlt and w/ wlt, the wing-body configurations except those of $x_w=3$ have better aerodynamic performance than the isolated wings. The drag coefficients are lower at zero-lift conditions and the lift coefficients and lift-to-drag ratios are higher at lifting conditions.

Figure 10 shows surface C_p distributions at zero-lift conditions (zero angles of attack) of the wing-body configurations w/o wlt and w/ wlt. Only the lower elements of the wings are shown to observe C_p distributions of inner surfaces of the wings. When $x_w=4$ and 4.5, which are affected by only the expansion waves, there are few differences of aerodynamic characteristics between the wings of the wing-body configurations w/o wlt and w/ wlt. On the other hand, there are noticeable differences when $x_w=3$ and 3.5, which are affected by not only the expansion waves but also the compression waves. Flow choking occurs on the wing-body configuration w/ wlt of $x_w=3$, which is widely exposed by the compression waves, and causes high drag. When $x_w=3.5$ w/ wlt, which is less effected by the compression waves, the area around the wingtip having high pressures causes low drag. These phenomena result in reflection of the compression waves from the winglet. When $x_w=3.5$ w/ wlt, the rear half of the surface around the wingtip is about double and causes reduction of drag. However, when the compression waves affect the wing with the winglet widely such as $x_w=3$ w/ wlt, they cause increase of drag with flow choking. Therefore, the condition of $x_w=3.5$ w/ wlt can be a sign of flow choking. In the cases without winglet, flow choking does not occur because increase of pressures due to the reflection of the compression waves does not occur. The drag reduction effects around the wingtip are also not expected. When $x_w=4$ and 4.5 both w/o wlt and w/ wlt, which are affected by only the expansion waves, remarkable characteristics can not be observed compared with the cases of $x_w=3$ and 3.5.

Figure 11 shows spanwise C_d distributions of the wings of both the wing-body configurations w/o wlt and w/ wlt at zero-lift conditions. First of all, the cases w/o wlt are discussed. When $x_w=3$ and 3.5, there are high C_d regions which are affected by the compression waves. It can be also confirmed that there are low C_d regions which are affected by fans of the expansion waves on all wing-body configurations. Next, the cases w/ wlt are discussed. The same tendency as the cases w/o wlt can be observed on all wing-body configurations. However, there is one unique characteristic on the wing-body configuration w/ wlt of $x_w=3.5$. The reflection of the compression waves at the winglet causes thrust force (low drag) near the winglet. The characteristic of the wing-body configuration w/ wlt of $x_w=3$ is not described because the flow choking occurs. In summary, on configurations both w/o wlt and w/ wlt, the areas affected by the compression waves have higher drag coefficients than the isolated wings except the reflection effects of the compression waves at the winglet. On the other hand, the areas affected by the expansion waves have basically higher or almost the same aerodynamic performance than isolated wings on all cases.

Figure 12 shows C_p distributions of the isolated wing w/ wlt, the wing-body configurations w/ wlt of $x_w=3.5$ and $x_w=4$ at zero-lift conditions (zero angles of attack). The remarkable phenomena can be observed on the wing-body configuration w/ wlt of $x_w=3.5$. In Fig. 12(b), C_p distributions at $y_w/b=0, 0.3$ and 0.7 are influenced by expansion waves (Here, y_w means spanwise coordinate from the wing root). Those at $y_w/b=1.1$ and 1.45 are influenced by compression waves, and that at $y_w/b=1.45$ is affected by the reflection of the compression waves from the winglet. The area affected by expansion waves ($0 < y_w/b < 0.8$) has lower drag, and the area affected by compression waves and without the reflection of them from the winglet ($0.8 < y_w/b < 1.4$) has higher drag, and the area near the winglet (around $y_w/b=1.5$) has lower drag. From Fig. 12(b) and (c), in expansion waves, the pressure jump of the first deflection of the leading edge of the wing (C_p of the front half) is lower than that of the isolated wing ($y_w/b=0, 0.3$ and 0.7 in Fig. 12(b) and all y_w/b in Fig. 12(c)). On the other hand, in compression waves, the pressure jump is higher than that of the isolated wing ($y_w/b=1.1$ and 1.45). The pressure levels of the rear half are not so different from those of the isolated wing compared to the pressure levels of the front half. As the result of it, aerodynamic performance can be improved when the wing is affected by expansion waves from the body. The high pressure of the rear half at $y_w/b=1.45$, which causes reduction of drag, can be also confirmed in Fig. 12(b).



Figure 7: Mesh visualization for analysis at cruise condition

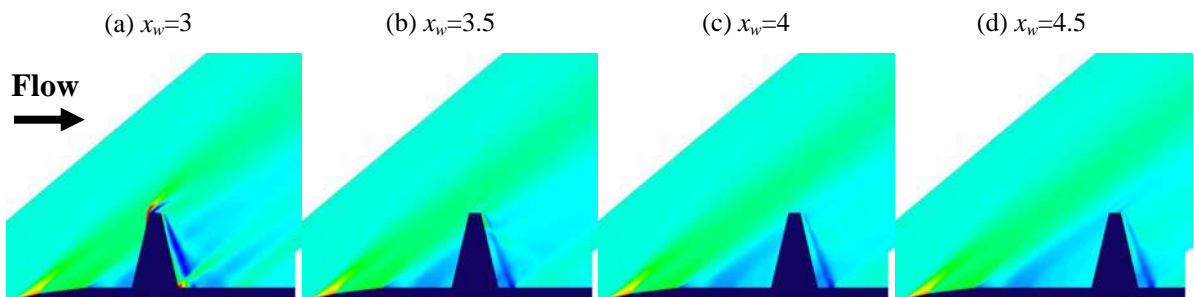


Figure 8: C_p visualizations of wing-body configuration w/ wlt at $z=0$ at zero-lift conditions (zero angles of attack)

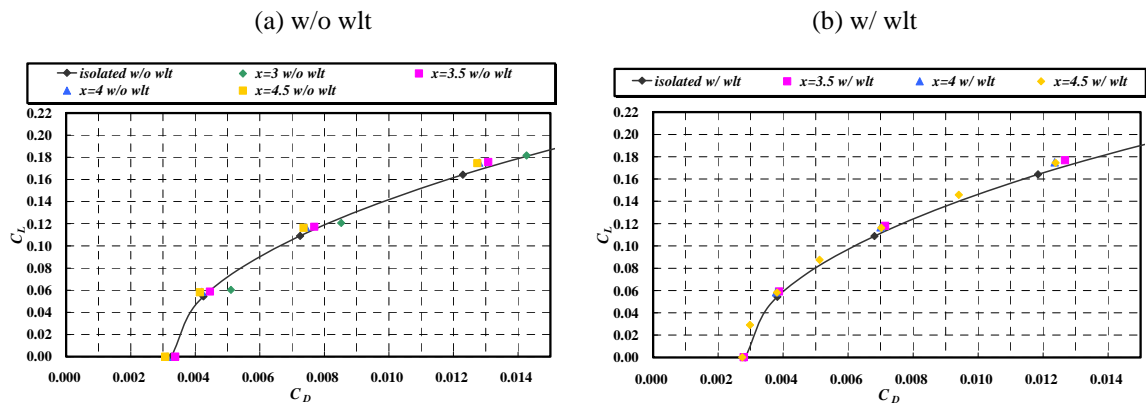


Figure 9: Drag polar diagrams of the wings of the wing-body configurations compared with the isolated wings

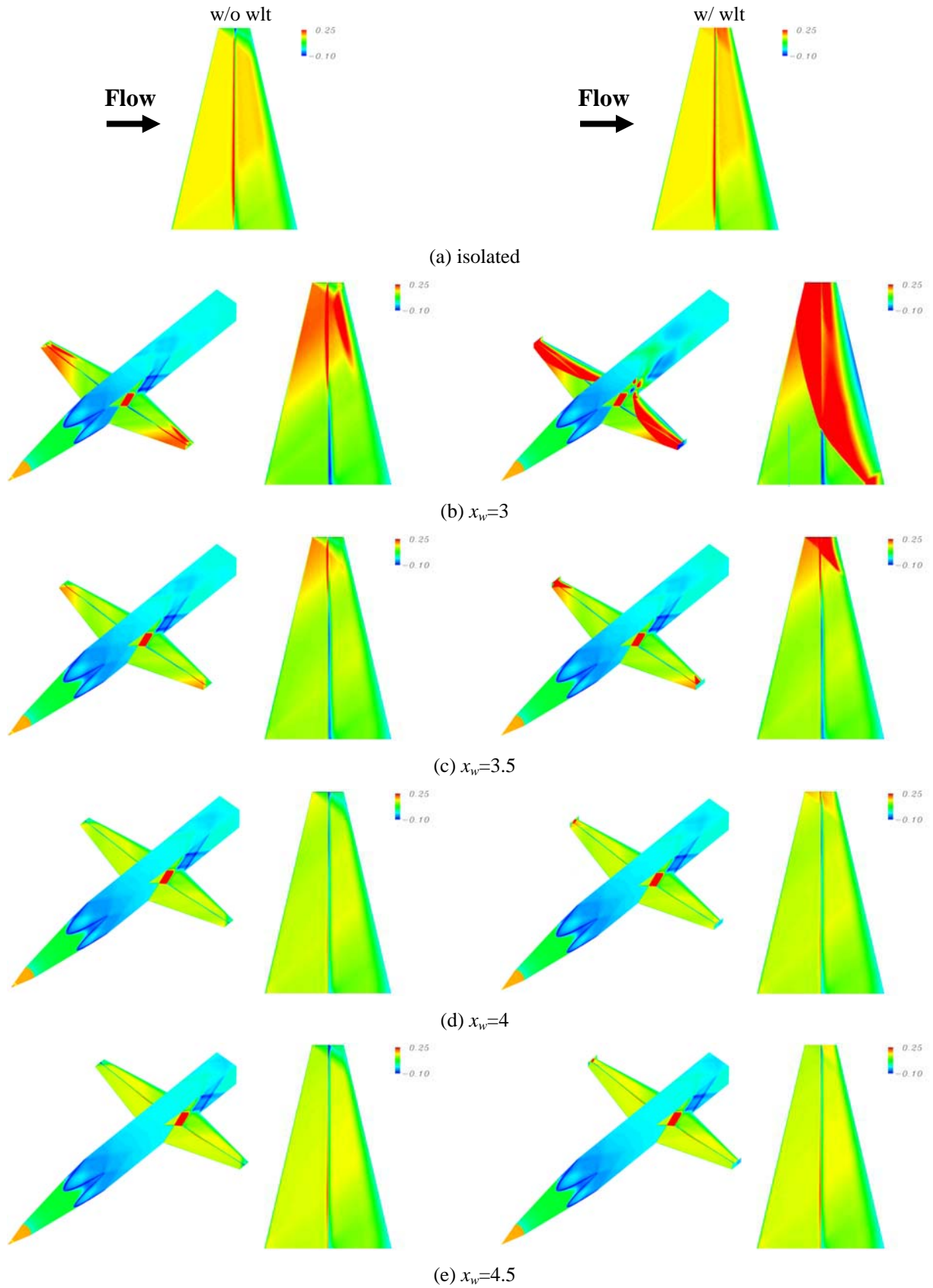


Figure 10: Surface C_p visualizations of isolated wings and wing-body configurations w/o wlt and w/ wlt at zero-lift conditions (zero angles of attack)

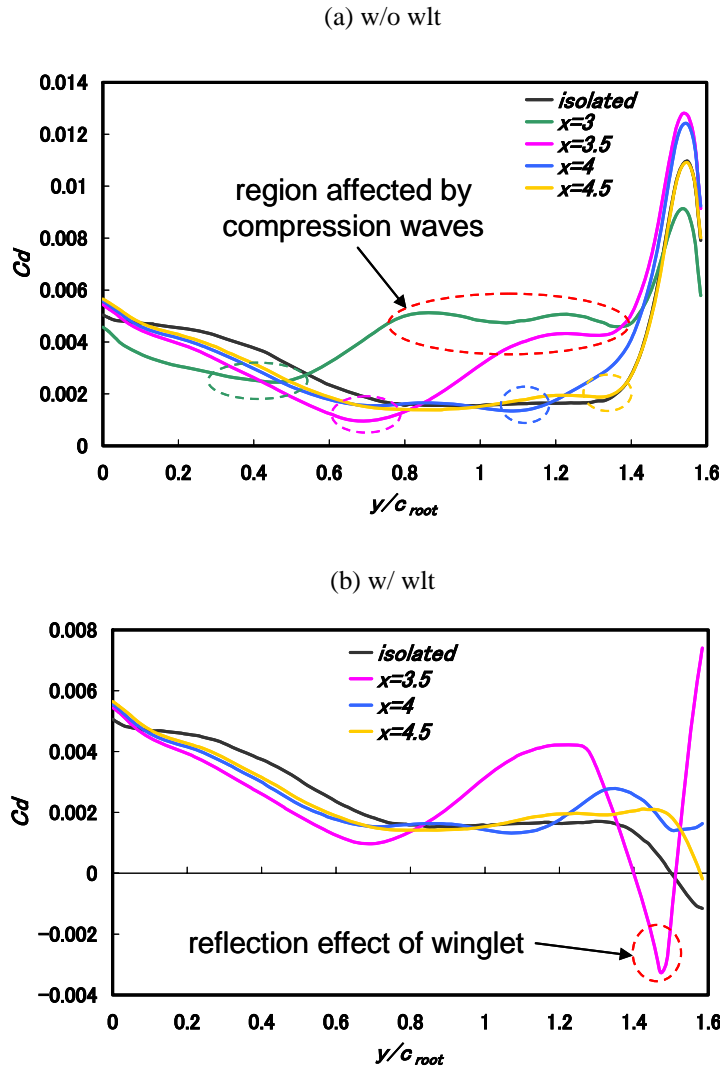


Figure 11: Spanwise C_d distributions at zero-lift conditions (zero angles of attack)

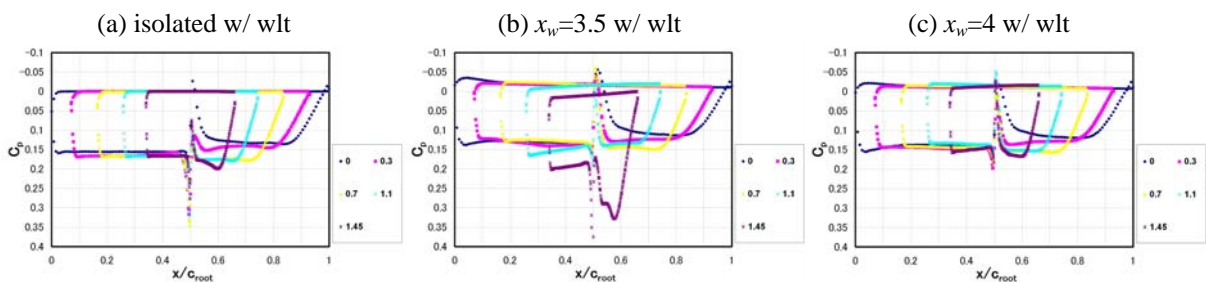


Figure 12: C_p distributions at some span stations at zero-lift conditions (zero angles of attack)

3.3 Aerodynamic characteristics at off-design conditions

In the previous section, it was confirmed that the expansion waves generated from the body can reduce aerodynamic performance and the compression waves reduce drag and increase lift coefficients partially by the reflection effects from the winglet. On design of supersonic biplanes, it is important to investigate aerodynamic characteristics at their off-design conditions. A flow choking occurs on supersonic biplanes at their off-design conditions. Especially when acceleration and deceleration of supersonic biplanes are considered, starting and unstaring problems, which can be observed in intake diffusers, occurs as hysteresis problems. Concerning on the starting problem, slats are useful to make the biplanes start at lower Mach number than a cruise Mach number [8].

On the other hand, the unstating problems are directly connected with stability at the cruise condition. The relations between the conditions that flow choking occur as unstating problem and that favorable interference of shock waves with expansion waves occurs are very close. In fact, the wing-body configuration w/ wlt of $x_w=3$ has flow choking and has high drag at the design Mach number.

Here, we discuss aerodynamic characteristics of the wing-body configurations at their off-design conditions. The configurations that were analyzed are as follow: (a) wing-body configuration w/ wlt of $x_w=3.5$, (b) wing-body configuration w/o wlt of $x_w=3.5$, (c) wing-body configuration w/ wlt of $x_w=4$, (d) wing-body configuration w/o wlt of $x_w=4$, (e) isolated w/ wlt and (f) isolated w/o wlt. Figure 13 shows mesh visualization for analysis at the off-design conditions. The number of nodes of each wing-body configuration is about 2.2 million. Figure 14 shows C_d vs M_∞ graph on deceleration stages. The unstating Mach numbers of the isolated wings w/o wlt and w/ wlt are 1.62 and 1.63, respectively. Those of the wing-body configurations except w/ wlt of $x_w=3.5$ are 1.60, which are lower than those of the isolated wings. The wing-body configuration w/ wlt of $x_w=3.5$ begins unstating at $M_\infty=1.69$, which is quite close to the cruise Mach number 1.7. The phenomenon at this condition is similar to that of the wing-body configuration w/ wlt of $x_w=3$ at the cruise condition. Figure 15 shows surface C_p visualizations around the unstating Mach numbers of the isolated wing w/ wlt, the wing-body configurations w/ wlt of $x_w=3.5$ and $x_w=4$. On the wing-body configuration w/ wlt of $x_w=3.5$, the flow choking spreads over the whole area of the wing from the wingtip unlike the phenomena in other cases.

There is a possibility of creating more lift and having better aerodynamic performance by utilizing the reflection of compression waves from other elements effectively. However, there is a disadvantage of stability on the cruise condition in terms of flow choking. As a result, the wing-body configurations w/ wlt of $x_w=4$ or $x_w=4.5$ are appropriate for aerodynamic performance at their design conditions and for stabilities on the unstating problems around the design conditions.



Figure 13: Mesh visualization for analysis at off-design conditions

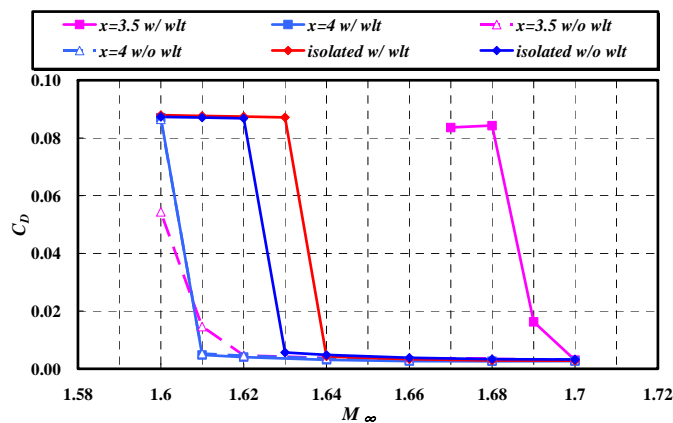


Figure 14: C_D characteristics of isolated wings and wings of wing-body configurations on deceleration stages

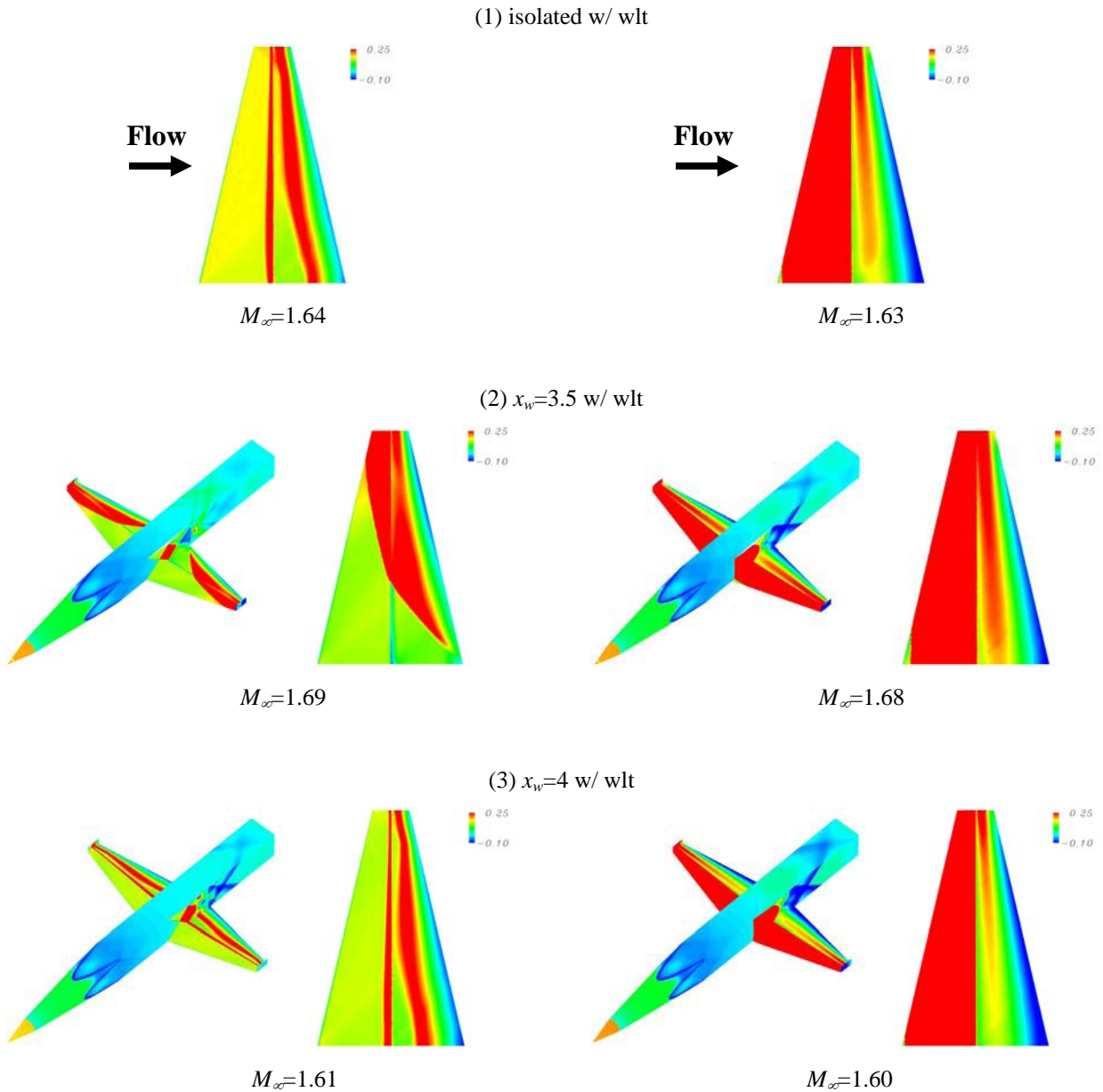


Figure 15: Surface C_p visualizations around unstating Mach numbers of isolated wing w/ wlt, wing-body configurations w/ wlt of $x_w=3.5$ and 4

4. Conclusions

For the feasibility study of wing-body configurations using a supersonic biplane concept, a wing-body configuration that generates strong shock waves and expansion waves was analyzed to assume that supersonic biplane wings are strongly affected by those waves. A wing-body configuration proposed by Odaka and Kusunose was used as a baseline wing-body configuration. We investigated how the strong shock waves and expansion waves generated from the body affect the aerodynamic performance and characteristics of supersonic biplane wings with changes of the position where the wings are attached to the body. Two types of biplane wings were used for these analyses: Busemann biplane without winglet, Busemann biplane with winglet. The planforms of these two wings are identical. They have a taper and their mid-chord lines are normal to the free-stream direction. The positions where the wings are attached to the body (x_w) are 0.3, 0.35, 0.4 and 0.45. When $x_w=0.3$, the wings are affected by compression waves widely. When $x_w=0.35$, they are affected by compression waves only around the wingtips. They also affected by expansion waves partially. When $x_w=0.4$ and 0.45, they are affected by only expansion waves.

The results of the biplane wing without winglet are firstly discussed. It was confirmed that the areas affected by shock waves had poor aerodynamic performance. On the other hand, the areas affected by expansion waves had better aerodynamic performance than the isolated wing. Next, the results of the biplane wing with winglet are discussed. When the wing is affected by only the expansion waves, $x_w=4$ and 4.5, the same trend as the case of without winglet was confirmed. However, when the wing is affected by compression waves, different phenomena from the case of without winglet were observed. When $x_w=3.5$, the compression waves affect the area around the wingtip and are reflected on the winglet. This phenomenon produces thrust forces around the wingtip and the aerodynamic performance of the wing becomes better than the isolated wing. When $x_w=3$, flow choking occurred at the wingtip and produces much amount of drag. This is also because high pressures are produced on the wide area of the inner surfaces of the wing due to the reflection of the compression waves at the winglet.

Aerodynamic characteristics at off-design conditions of the wing-body configurations were also investigated. For the stability around the cruise condition, it is especially important to take unstating problems into account. Quasi-unsteady simulations were conducted to the isolated wings and the wing-body configurations to simulate deceleration from the cruise Mach number 1.7. The wing-body configuration with winglet of $x_w=3.5$ began unstating at $M_\infty=1.69$. The phenomenon at this Mach number is similar to that of the wing-body configuration with winglet of $x_w=3$ at the cruise condition. The other configurations have wide stable region for unstating problems. The unstating Mach numbers are 1.60, which are lower than those of the isolated wings. Those of the isolated wings w/o wlt and w/ wlt are 1.62 and 1.63, respectively. In conclusion, it is better for biplane wings to be affected by expansion waves than not to be affected both at design and off-design conditions. When supersonic biplane wings are affected by compression waves, aerodynamic performance of the wings can be improved by using a winglet effectively, while wings are easy to cause unstating around the cruise Mach number.

References

- [1] Odaka, Y., and Kusunose, K., "Interference Effect of Body on Supersonic Biplane Wings," 40th Fluid Dynamics Conference/Aerospace Numerical Simulation Symposium 2008, Paper 1B10, June 2008, pp87-90. (In Japanese)
- [2] Odaka, Y., and Kusunose, K., "Effects of a Bulky Fuselage on Aerodynamic Characteristics of Supersonic Biplane Wings," Proceeding of. The 40th JSASS Annual Meeting, April, 2009, pp.68-73. (In Japanese)
- [3] Odaka, Y., and Kusunose, K., "A Fundamental Study for Aerodynamic Characteristics of Supersonic Biplane Wing and Wing-Body Configurations," Journal of The Japan Society for Aeronautical and Space Sciences, Vol. 57, No. 664, 2009, pp.217-224. (In Japanese)
- [4] Nakahashi, K., Ito, Y., and Togashi, F., "Some Challenge of Realistic Flow Simulations by Unstructured Grid CFD," International Journal for Numerical Methods in Fluids, Vol.43, 2003, pp. 769-783.
- [5] Ito, Y., and Nakahashi, K., "Surface Triangulation for Polygonal Models Based on CFD Data," International Journal for Numerical Methods in Fluids, Vol.39, Issue 1, 2002, pp. 75-96.
- [6] Sharov, D., and Nakahashi, K., "Reordering of Hybrid Unstructured Grids for Lower-Upper Symmetric Gauss-Seidel Computations," AIAA Journal, Vol.36, No.3, 1998, pp. 484-486.
- [7] Ito, Y. and Nakahashi, K. "Unstructured Mesh Generation for Viscous Flow Computations," Proceedings of the 11th International Meshing Roundtable, Ithaca, NY, 2002, pp.367-377.
- [8] Maruyama, D., Matsuzawa, T., Kusunose, K., Matsushima, K., and Nakahashi, K., "Consideration at Off-design Conditions of Supersonic Flows around Biplane Airfoils," AIAA Paper 2007-0687, January 2007.